Contents list available at IJRED website

Int. Journal of Renewable Energy Development (IJRED)

Journal homepage: http://ejournal.undip.ac.id/index.php/ijred

Short Communication

Preparation of Anode Material for Lithium Battery from Activated Carbon

Sumrit Mopoung[a*], Russamee Sitthikhankaew[b], Nantikan Mingmoon[a]

[a]Chemistry Department, Faculty of Science, Naresuan University, Phitsanulok, Thailand

[b]School of Renewable Energy and Smart Grid Technology, Naresuan University, Phitsanulok, Thailand

ABSTRACT. This research study describes the preparation of corncob derived activated carbon to be used as anode material for the preparation of lithium ion battery. The corncob was activated at 900 °C for 3 hours with KOH used in a 1:3 weight ratio. The final product was analyzed for chemical, physical, and electrical properties. The results show that the activated carbon is amorphous and contains some graphitic carbon with interconnected nano-channels. Furthermore, carboxyl functional groups were detected on the surface of the activated carbon product. The observed morphological characteristics in terms of surface area, total pore volume, micropore volume, and average pore size are 1367.4501 m^2/g, 0.478390 cm^3/g, 0.270916 cm^3/g, and 2.10872 nm, respectively. In addition, the product also exhibits low electrical resistance in the range 0.706 Ω-1.071 Ω. Finally, the specific discharge capacities at the 1st and the 2nd cycles of the corncob derived activated carbon anode material were 488.67mA h/g and 241.45 mA h/g, respectively with an average of about 225 Ah/kg between the 3rd cycle and the 5th cycle. The average specific charge capacities/specific discharge capacities at increasing charging rate of 0.2C, 0.5C, 1C, 2C, and 5C were approximated 190 mA h/g, 155 mA h/g, 135 mA h/g, 120 mA h/g, and 75 mA h/g, respectively, with 100% Coulombic efficiency in all 5 cycles. It was shown that the corncob derived activated carbon anode material has a relatively high rate capability, high reversibility, and rapid and stable capacity when compared to the general of biomass-derived carbon.

Keywords: Activated carbon, anode material, corncob, lithium ion battery

Article History: Received: 10th Sept 2020; Revised: 18th Oct 2020; Accepted: 21st Oct 2020; Available online: 25th Oct 2020
How to Cite This Article: Mopoung, S., Sitthikhankaew, R., and Mingmoon, N. (2021). Preparation of Anode Material for Lithium Battery from Activated Carbon. *Int. Journal of Renewable Energy Development*, 10(1), 91-96
https://doi.org/10.14710/ijred.2021.32997

1. Introduction

Lithium ion batteries are being used in large-scale for electric vehicles, hybrid electric vehicles, advanced power load levelling of smart grids, and modern mobile technology. In addition, the rechargeable lithium-ion battery has been commercialized to meet the sustained market's demands (Sharma, Panwar, & Tripathi, 2020). It also have revolutionized consumer electronics (Gong *et al.* 2016). It contains 2 electrodes, anode and cathode, where the anode provides the electron capacity and the cathode delivers the electron power density (Song *et al.* 2016; Iwai *et al.* 2019). The electrode materials of lithium ion battery are composed of conductive carbon materials, binding agents, and inorganic compounds (Zhang, Hu, & Chen, 2013). To increase the capacitance of lithium ion batteries, it is designed with extremely small distances that separate the opposite charges (the electric double-layer) and highly porous electrodes that embody very high surface-area (Pandolfo and Hollenkamp, 2006). In this research, we focus on the preparation and characterization of a potential anode material. Thus, only the anode materials are discussed below. The desired characteristics of the anode of lithium ion battery are high number of micropores, to enable reversible capacity, and mesopores, to provide the channels for Li^+ ion transport and enhance the infiltration of the electrolyte (Zhang, Hu, & Chen, 2013). In general, the anode materials are based on C, Si, Sn, or their alloys/compounds, and transition metal oxides (Zhang, Hu, & Chen, 2013). However, carbon materials are the materials of choice to prepare the anode. This is because of their favourable properties such as high conductivity, high surface-area, good corrosion resistance, high temperature stability, controlled pore structure process ability, and compatibility in composite materials. In addition, carbon materials have a relatively low cost (Pandolfo & Hollenkamp, 2006). These properties will enhance the high specific capacity of the anode (Song *et al.* 2016). The carbon material types that have been chosen for anode construction are activated carbon, carbon black, carbon aerogels, carbon fiber, glassy carbon, and carbon nanostructures (Pandolfo & Hollenkamp, 2006). The activated carbon could improve the electrochemical properties because of its high surface area and pore volume, excellent electronic conductivity, and strong adsorption capacity (Zhang, Hu, & Chen, 2013). The

* Corresponding author: sumritm@nu.ac.th

precursors for activated carbon materials are mostly carbon rich organics, which can even be derived from renewable and sustainable resources to prevent global warming (Valentini, 2015). Therefore, the activated carbon from biomass was collected for anode preparation in this research. Subsequently, the produced anode material is environmentally- friendly made in a green, low cost, and facile way to provide carbon electrode of electrical double-layer capacitors (Pode, 2016).

This research studies anode preparation for lithium ion battery from corncob derived activated carbon. The chemical and physical properties of corncob derived activated carbon were characterized to determine the functional surface groups, structure, morphology, elemental composition, electrical resistance, and electrical conductivity. Charge and discharge capacity at different rates for the prepared anode were measured as well to determine the capability rate, specific charge/discharge capacity, reversibility, and stable capacity.

2. Materials and Methods

2.1 Preparation of activated carbon

The corncob was dried in an oven (SL 1375 SHEL LAB 1350 FX) at 110°C for 3 h. The dried corncob was mixed with KOH (UNID Co., Ltd; Korea) in a corncob:KOH weight ratio of 1:3 weight ratio. Distilled water, 20 %-vol relative to the weight of the mixed sample, was added and the resulting mixture was dried again at 110°C overnight. KOH was used as a typical chemical reagent to induce porosity by partial oxidation at high activation temperature. The dried mixed sample was placed in a porcelain crucible with a lid and activated at 900°C by a furnace (Fisher Scientific Isotemp® Muffle Furnance, USA) under nitrogen atmosphere with heating rate 10°C/min. The sample was exposed to the final temperature for 0.5 h and then cooled down to room temperature. The final product was washed with 1 M HCl (Assay 37%; Merck Germany) and dried at 110°C for 3 h. The dried sample was weighted by analytical balance (Sartorious; Germany) for percent yield determination. Fourier transform infrared spectrophotometry (FTIR, Spectrum GX, Perkin Elmer), Raman spectroscopy (Bruker, MultiRAM), scanning electron microscopy equipped with energy-dispersive X-ray spectrometer (SEM-EDS, Mode LEO 1455 VP, LEO Electron Microscopy Ltd, England), transmission electron microscopy(TEM, Phillips, Tecnai12, Netherland), X-ray diffraction (XRD, PW 3040/60 X·Pert PRO Console, Philips, Netherland), and Brunaure-Emmett-Teller(BET, Micromeritics TriStar II) were used for characterization of the corncob derived activated carbon. The electrochemical properties of the corncob derived activated carbon were also measured by SourceMeter® (Keithley, 6430·s Remote preamp).

2.2 *Preparation of test pieces for electrical property measurement*

Corncob derived activated carbon was ground to a size of 80 mesh and then weighed (1.5 g) and mixed with 3-4 drops of polyvinyl alcohol (BF17W; Ajax Finechem Pty Ltd) binder. The homogeneous mixed sample was pressed by hydraulic press into a disc shape with a diameter and thickness of 2 mm and 1.5 mm, respectively, and then dried at 50°C for 24 h under vacuum before testing.

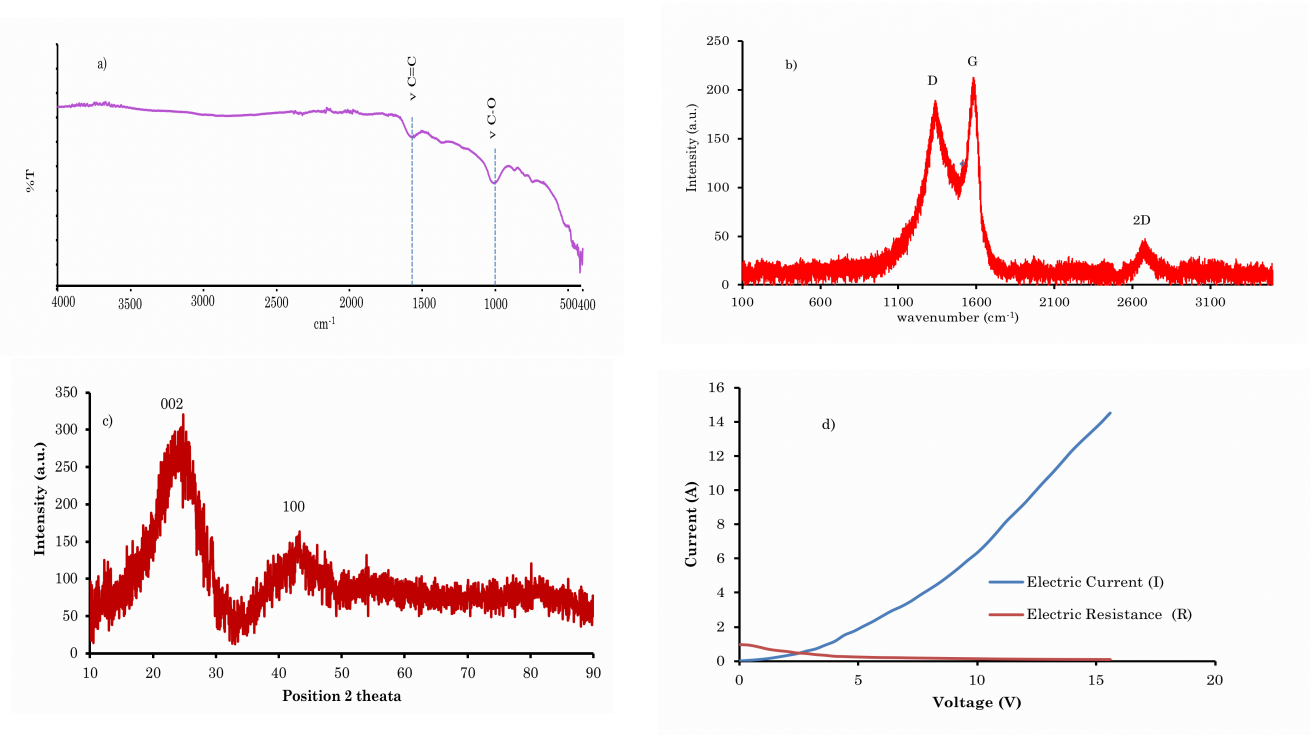

Fig.1 Characterization results for corncob derived activated carbon (a)FTIR transmission spectrum (b) Raman spectrum, (c) XRD spectrum, and (d) electrochemical properties

The electrical properties of the dried disc sample that were measured and evaluated are electric conductivity and resistance. The measurements were carried out by applying electrical potential (0-16 V, V) and electrical current (0-15 A, I) by SourceMeter® at room temperature. The electrical resistance (R) was calculated by Ohm's Law (R=V/I).

2.3 Preparation of anode and electrochemical efficiency measurement

The corncob derived activated carbon was also ground to 80 mesh for anode preparation. It was mixed with conductive carbon black (Super P) and binder solution (3.64 wt-% polyvinylidene fluoride (Aldrich) and 96.36 wt-% N-methyl-2pyrrolidone) in ratio of 79.74 wt-% of corncob derived activated carbon : 10.34 wt-% Super P: 9.92 wt-% binder solution. The well-proportioned slurries were deposited on aluminium foil (as the counter electrode) and dried in a vacuum oven at 80°C for 12 hours to achieve N-methyl-2pyrrolidone evaporation. After drying, the dried mixed material was assembled into coin cells in an argon-filled glove box. Microporous polymer (Celgard 2400) is used as a separator for construction of the coin-type cells. The electrochemical testing of the corncob derived activated carbon anode was performed in a Glove box under a flow of argon to inhibit oxidation of the lithium metal foil to lithium oxide (Li_2O), which affects the electrical efficiency of the lithium metal foil as a cathode. The capability rate was determined by galvanostatic cycling method where various values of the electrical current were measured to provide the voltage that is derived from the redox reaction of activated carbon at charge and discharge rates of 0.1C, 0.2C, 0.5C, 1C, 2C, and 5C for 5 cycles, over the electric potential range between of 0.02 and 2.5 V at a scan rate of 0.1 mV/s.

3. Result and discussion

3.1 Characterization of activated carbon

3.1.1 Percent yield

The percent yield of corncob derived activated carbon prepared by activation at 900°C under N_2 atmosphere is 12.94 ± 0.04%. It is rather low, because the corncob has a soft and light texture. Moreover, KOH had increased the level of oxidation of corncob at the activation temperature of 900°C. Therefore, the organic matter such as hemicellulose, cellulose, lignin, and some carbon in the corncob underwent quite high thermal degradation and partial oxidation during carbonization and KOH activation.

3.1.2 FTIR transmission spectrum of activated carbon

Fig 1a shows the FTIR transmission spectrum of the corncob derived activated carbon. It can be seen that some carboxylic surface group were grafted onto the corncob derived activated carbon as demonstrated by the quite weak broad band at about 1100 cm^{-1} (Han *et al.* 2014). This oxygen-containing functional surface group could improve the wettability of the electrode materials in aqueous electrolyte and enhance the capacitance through additional Faradaic reactions (Xing *et al.* 2015). However, it can also affect the resistivity of activated carbon, which is the barrier for transfer electrons (Pandolfo & Hollenkamp, 2006). Another very weak peak is located at about 1600 cm^{-1} and it corresponds to the olefin conjugated with aromatic ring or double bonds.

These results suggest that the hydroaromatics present in corncob have condensed to form aromatic ring structures by dehydrogenation at carbonization temperatures of 400-500°C. This indicates that a three-dimensional network has formed in the activated carbon, which gives this material good properties for the transfer of electrons, thus making in an interesting anode. Both aromatic rings and surface carboxyl groups are usually formed from cleavage of intra- molecular dehydration during carbonization and activation (Xin *et al.* 2015), respectively.

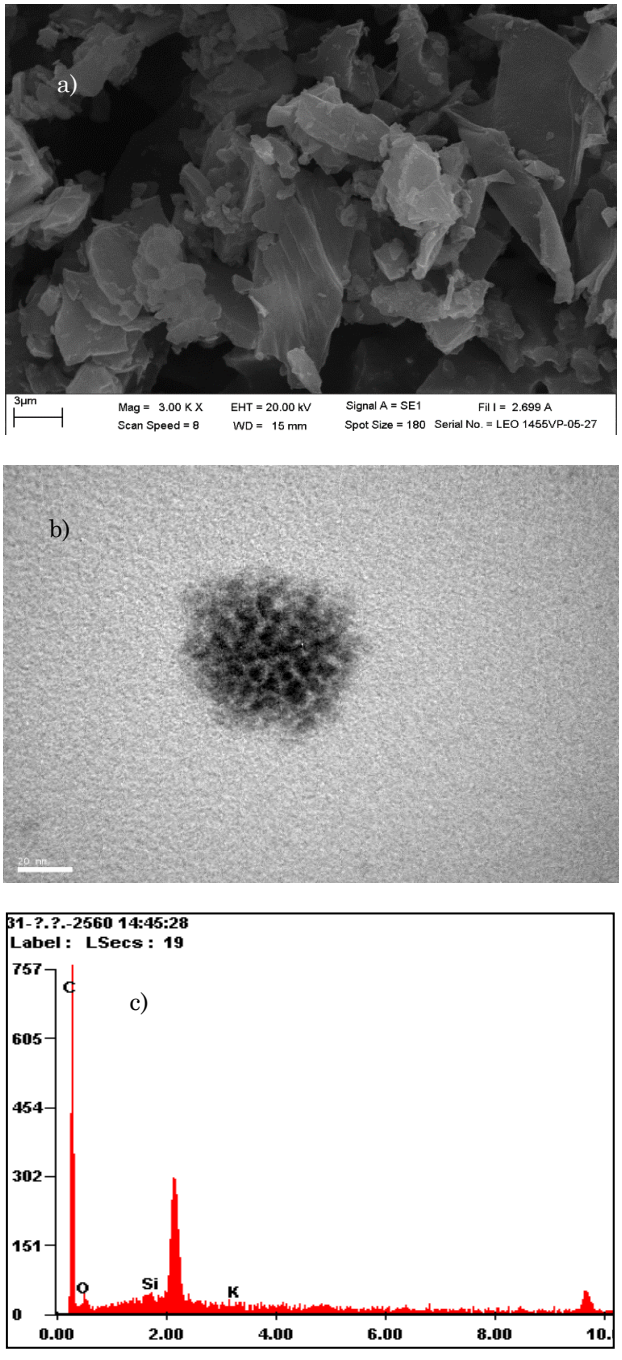

Fig. 2. Microstructural characterization by (a)SEM (3000x), (b) TEM (360000x) and elemental composition by (c) EDS of corncob derived activated carbon.

3.1.3 Raman bands information of activated carbon

Fig 1b shows the Raman bands of corncob derived activated carbon at 1350 cm^{-1}, 1585 cm^{-1}, and 2710 cm^{-1}, which correspond to the D band, G band, and D_2 band, respectively. The D band reveals the presence of sp^3 hybridized carbon atoms in amorphous and quasi-crystalline forms of carbon materials, while the G band reveals the in-plane vibrations of the sp^2 carbon atoms of crystalline graphite (Wu *et al.* 2016; Zhu *et al.* 2016). It is assumed that the dehydrogenation of hydroaromatics has occurred and aromatic rings assembled in the reducing atmosphere, which resulted in the formation of graphene sheet of crystalline graphite. The value of I_D/I_G peak intensity ratio is 0.917. This indicates that the activated carbon is formed from partial crystallization of few layers of graphene, which could improve the electrical conductivity of the carbonaceous material (Ru *et al.* 2016). This is further confirmed by the weak D_2 band at 2710 cm^{-1}, which is related to the growth of crystalline 2D graphene phase. This is consistent with the reported results for high temperature activation at 900°C resulting in increased graphitization degree (Xin *et al.* 2015). On the other hand, KOH activation results in amorphous carbon formed by partial oxidation and grafting of functional surface groups on the surface of corncob derived activated carbon after KOH activation, which was reported for porous carbon made soybean residue (Chen *et al.* 2016) and microalgae (Ru *et al.* 2016). In these two instances the I_D/I_G value was less than 1. These results could be beneficial for effective charge transfer and electron capacity, which should improve the storage ability of the anode.

3.1.4 XRD spectrum of activated carbon

The XRD pattern of the corncob derived activated carbon is shown in Fig. 1d. The two main broad XRD bands are located at 2θ=24.5° and 43° and are associated with the (002) crystal planes of parallel-stacked graphene sheets and the (100) crystal planes of sp^2 carbons of a honeycomb structure (Han *et al.* 2014), respectively. This result demonstrates the presence of both graphitic carbon and amorphous carbon in the activated carbon formed during carbonization and activation by KOH at 900°C. Furthermore, this corresponds to the Raman spectrum described above. It is assumed that the formation of graphitic carbon is due to the condensation of small aromatic rings by dehydrogenation of hydroaromatics at the high carbonization temperature, which is consistent with the report of Xin *et al.* (2015). During the activation stage, some graphene sheets from corncob carbon, which formed during the carbonization stage, were destroyed by partial oxidation in the presence of KOH. This has resulted in the presence of both graphitic carbon and amorphous carbon characteristics in the corncob derived activated carbon.

3.1.5 Electrochemical Properties

Fig. 1d shows electrical resistance, in response to varied the electrical voltage (0-16 V) and electrical current (0-15 A), of the corncob derived activated carbon. It can be seen that the electrical resistance was relatively low (range between 0.706 and 1.071 Ω) and stable throughout the operation.

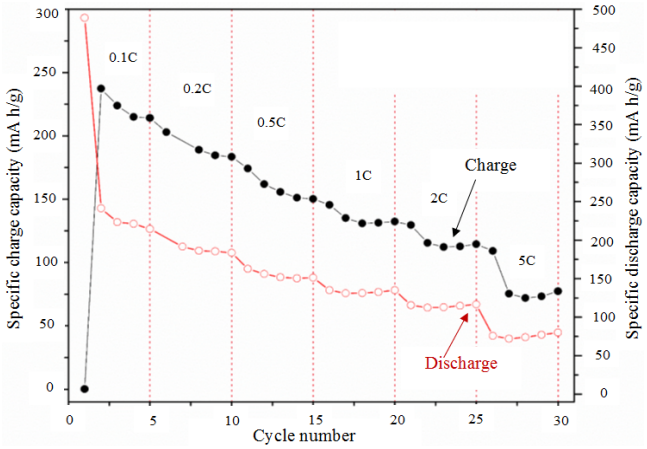

Fig. 3 Specific charge capacity and specific discharge capacity of lithium ion battery prepared using corncob derived activated carbon as anode material at charge and discharge rates of 0.1C,0.2C, 0.5C, 1C, 2C and 5C.

This is due to the low content of surface functional groups and presence of some amount of structurally ordered graphitic carbon in the corncob derived activated carbon, which was confirmed by FTIR, Raman spectrum, and XRD results. The low electrical resistance of the activated carbon resulted in good electrical conductivity, although increasing the electrical potential and electrical current. This observed property has a positive effect on the electrical conductivity of the activated carbon to be used as an anode of lithium ion battery for electron storage and rate charging.

3.1.6 Morphology and elements composition of activated carbon

The SEM image (Fig. 2a) of corncob derived activated carbon after washing with 1 M HCl solution shows opened pore channels. A bent plate and small pieces were observed on the surface of the activated carbon. It has been shown that there is a tendency for the formation of graphitic carbon, which will result in improved electrical conductivity of the activated carbon. The results of TEM characterization with magnification of 360000 times (Fig. 2b) show that the corncob derived activated carbon has an amorphous structure and some graphitic carbon with interconnected nano-channels in the activated carbon. The results of the EDS analysis (Fig. 2c) show that the C content is dominant (86.69 wt-%), along with a small amount of O (11.23 wt-%), which corresponds to the results of FTIR spectrum. Furthermore, the O:C atomic ratio in the activated carbon was calculated and it is only 0.0973, which is attributed to the extensive decomposition of oxygen containing functional surface groups on raw corncob at high temperature. This ratio is similar to activated carbon from made lignite and activated with KOH (Xing *et al.* 2015). There is also a very small amount of Si (1.33 wt-%) and K (0.75 wt-%). The silicon content likely originates form plant absorption from the soil through the roots and subsequent accumulation in the corncobs, which is detected even after washing with HCl solution. The K content likely came from the reaction of $6KOH + 2C \rightarrow 2K_2CO_3 + 2K + 3H_2$. Followed by the K_2CO_3 reduction with carbon to form K, K_2O, CO, and CO_2 (Xing *et al.* 2015). The porosities of the activated carbon were

also formed by these reactions resulting in increased surface area, pore volume, and microporosity.

3.1.7 Surface area and pore volume of activated carbon

The corncob derived activated carbon has values of surface area, total pore volume, micropore volume, and average pore size of 1367.4501 m^2/g, 0.478390 cm^3/g, 0.270916 cm^3/g, and 2.10872 nm, respectively. This is due to the KOH activation at high temperature. The KOH penetration into crystalline graphene results in edge-enriched porous carbon. Furthermore, corncob derived activated carbon also has total volume and total area in pores of 0.38731 cm^3/g and 79.190 m^2/g, respectively. In addition, the micropore volume is 56.63% of total pore volume, which shows that the remaining pore volume corresponds to mesopore (37.10%) and macropore (6.27%). These characteristics, especially micropore volume, are good for improving the storage ability of the anode. This is because the high volume is advantageous for high performance lithium ion batteries, while micropore and open pore are suitable for electron transport and lithium ion diffusion, which is beneficial for the reversible specific capacity. In addition, electrolyte can easily penetrate into the interior of the electrode material through the mesopore and macropore (Huang *et al.* 2016). The total volume and total area in pores of activated carbon are good characteristics for electrode/electrolyte contraction and rapid mass transport of lithium ions and electron transport (Zhang, Hu, & Chen, 2013).

3.2 Performance testing of corncob derived activated carbon as anode material

Figure 3 provides the specific charge capacity and specific discharge capacity of lithium ion battery prepared with the corncob derived activated carbon as anode material. At the rate of charge and discharge of 0.1C, the specific discharge capacity at the 1st and the 2nd cycle of the discharging were 488.67 mA h/g and 241.45 mA h/g, respectively with an average of about 225 mA h/g from the 3rd to the 5th cycle. While the specific charge capacity at the 1st and 2nd cycle of charging were 0.04 mA h/g and 237.42 mA h/g, respectively. The Coulombic efficiency during the 1st cycle of charging at 0.1C rate was 0.01% with almost irreversible initial loss, which is due to the irreversible reaction and capacity loss caused by the formation of the solid electrolyte interphase layer (Zhang *et al.* 2007). However, the Coulombic efficiency was 98. 33% during the 2nd cycle, while Coulombic efficiencies from the 3rd to the 5th cycle were 100%, indicating a highly reversible lithium insertion and extraction. During the charge and discharge cycles carried out at the rate of 0.2C, specific charge capacity and specific discharge capacity were slightly decreased in comparison to the charge/discharge rate of 0.1C. Furthermore, the Coulombic efficiency from the 1st to 5th cycle was 100%, which was also observed for experiments using 0.5C to 5C of charge/discharge rate. This is associated to the limited transportation of the electrolyte ions in the anode materials with a fast capacity rate (Xing *et al.* 2015). However, on closer inspection it was determined that the specific charge capacity and specific discharge capacity were slightly increased after 3rd cycle of 1C to 5C charge/discharge rate, while maintaining the 100% of Coulombic efficiency. This result indicates that the stable capacity of the activated carbon derived anode is rapidly established (Zhang *et al.* 2007). The average specific charge capacities/specific discharge capacities observed at 0.2C, 0.5C, 1C, 2C, and 5C rates were approximately 190 mA h/g, 155 mA h/g, 135 mA h/g, 120 mA h/g, and 75 mA h/g, respectively, which is constant in all 5 cycles with 100% Coulombic efficiency. This indicates that the microporosity of the activated carbon derived anode material can result in highly reversible and stable capacity (Zhang *et al.* 2007). The highly stable capacity is related to the pores of the activated carbon containing a wide range of pore types from micropores to macropores, interconnected porous channels, high surface area, and oxygen-containing surface group. The high microporosity and surface area can result in the high capacity for charge storage, while the interconnected porous channels of meso-macropores could enhance the diffusion of lithium ions and electron transport (Zhu *et al.* 2016). Finally, the oxygen containing surface groups can improve the wettability for charge storage (Xing *et al.* 2015). Thus, the corncob derived activated carbon anode material exhibits a relatively high rate capability (488.67 mA h/g) as well as reversible, rapid, and stable capacity with 100% Coulombic efficiency. This represents a significant improvement in comparison with the general of biomass derived carbon materials with only 65-85% of Coulombic efficiency and < 400 mA h/g (Rios *et al* 2018).

4. Conclusion

Activated carbon from corncob was prepared with KOH as the activating agent at 900°C under N_2 atmosphere and washed by HCl solution. The percent yield of final product was 12.94 ± 0.04%. The resulting material has 86.69 wt-% C content and shows the characteristics of both graphitic carbon and amorphous carbon as well as the presence of some carboxylic surface groups. Interconnected nano-channels and opened pore channels remain in the final product were also after HCl washing with values of surface area, total pore volume, micropore volume and average pore size of 1367.4501 m^2/g, 0.478390 cm^3/g, 0.270916 cm^3/g and 2.10872 nm, respectively. In addition, the obtained material shows a relatively low and stable electrical resistance in the range between 0.706 and 1. 071 Ω for 0-16 V of electrical potential. These characteristics of the corncob derived activated carbon are suitable for the preparation of anodes of lithium ion batteries. The capability rate of the activated carbon derived anode material was measured at different charge and discharge rates from 0.1C to 5C. The specific discharge capacities at 0.1C rate of the 1st and the 2nd cycle were 488.67 mA h/g and 241.45 mA h/g, respectively. While the specific charge capacities at the 1st and 2nd cycle of charging were 0.04 mA h/g and 237.42 mA h/g, respectively. This indicates that an irreversible reaction and capacity loss, which are caused by the formation of the solid electrolyte interphase layer, is also taking place. For the charge/discharge rates in the range from 0.2C to 5C, specific charge capacity and specific discharge capacity decrease with increasing rate. The average specific charge capacities/specific discharge capacities at 0.2C, 0.5C, 1C, 2C and 5C were approximately 190 mA h/g, 155 mA h/g, 135 mA h/g, 120 mA h/g, and 75 mA h/g, respectively. These values remain constant in all 5 cycles while also maintaining 100% Coulombic efficiency. This shows that the corncob derived activated carbon anode material has a relatively high rate

capability, high reversibility, and quickly established and stable capacity in comparison to the general of biomass derived carbon materials.

Acknowledgments

The authors acknowledge the National Science and Technology Development Agency for partial financial support and Science lab center, Faculty of Science, Naresuan University for all of the analysis.

References

Chen, F., Yang, J., Bai, T., Long, B., & Zhou, X. (2016). Biomass waste- derived honeycomb-like nitrogen and oxygen dual-doped porous carbon for high performance lithium- sulfur batteries. *Electrochimica Acta*, *192*, 99–109.

Gong, C., Xue, Z., Wen, S., Ye, Y., & Xie, X. (2016). Advanced carbon materials/olivine $LiFePO_4$ composites cathode for lithium ion batteries. *Journal of Power Sources*, *318*, 93-112.

Han, S.-W., Jung, D.-W., Jeong, J.-H., & Oh, E.-S. (2014). Effect of pyrolysis temperature on carbon obtained from green tea biomass for superior lithium ion battery anodes. *Chemical Engineering Journal*, *254*, 597–604.

Huang, Y., Lin, Z., Zheng, M., Wang, T., Yang, J., Yuan, F., Lu, X., Liu, L., & Sun, D. (2016). Amorphous Fe_2O_3 nanoshells coated on carbonized bacterial cellulose nanofibers as a flexible anode for high- performance lithium ion batteries. *Journal of Power Sources*, *307*, 649-656.

Iwai, K., Tamura, T., Nguyen, D.T., & Taguchi, K. (2019). The development of a flexible battery by using a stainless mesh anode. *International Journal of Renewable Energy Development*, *8*(*3*), 225-229.

Pandolfo, A.G., & Hollenkamp, A.F. (2006) Carbon properties and their role in supercapacitors. *Journal of Power Sources*, *157*, 11–27.

Pode, R. (2016). Potential applications of rice husk ash waste from rice husk biomass power plant. *Renewable and Sustainable Energy Reviews*, *53*, 1468–1485.

Rios, C.D.M.S., Simone, V., Simonin, L., Martinet, S., & Dupont, C. (2018). Biochars from various biomass types as precursors for hard carbon anodes in sodium-ion batteries. *Biomass and Bioenergy, 117,* 32-37.

Ru, H., Bai, N., Xiang, K., Zhou, W., Chen, H., & Zhao, X.S. (2016). Porous carbons derived from microalgae with enhanced electrochemical performance for lithium- ion batteries. *Electrochimica Acta*, *194*, 10–16.

Sharma, S., Panwar, A.K., & Tripathi, M.M. (2020). Investigation of electrochemical, thermal and electrical performance of 3D lithium-ion battery module in a high-temperature environment. *International Journal of Renewable Energy Development, 9*(*2*), 151-157.

Song, H., Fu, J., Ding, K., Huang, C., Wu, K., Zhang, X., Gao, B., Huo, K., Peng, X., & Chu, P. K. (2016). Flexible Nb_2O_5 nanowires/ graphene film electrode for high performance hybrid Li-ion supercapacitors. *Journal of Power Sources*, *328*, 599-606.

Valentini, L. (2015). Bio- inspired materials and grapheme for electronic applications. *Materials Letters*, *148*, 204–207.

Wu, F., Huang, R., Mu, D., Wu, B., & Chen, Y. (2016). Controlled synthesis of graphitic carbon- encapsulated a- Fe_2O_3 nanocomposite via low-temperature catalytic graphitization of biomass and its lithium storage property. *Electrochimica Acta*, *187*, 508–516.

Xin, S., Yang, H., Chen, Y., Yang, M., Chen, L., Wang, X., & Chen, H. (2015). Chemical structure evolution of char during the pyrolysis of cellulose. *Journal of Analytical and Applied Pyrolysis*, *116*, 263-271.

Xing, B.-L., Guo, H., Chen, L.-J., Chen, Z.-F., Zhang, C.-X., Huang, G.-X., Xie, W., & Yu, J.-L. (2015). Lignite-derived high surface area mesoporous activated carbons for electrochemical capacitors. *Fuel Processing Technology*, *138*, 734–742.

Zhang, K., Hu, Z., & Chen, J. (2013). Functional porous carbon-based composite electrode materials for lithium secondary batteries. *Journal of Energy Chemistry*, *22*, 214–225.

Zhang, Y., Zhang, F., Li, G.D., & Chen, J.-S. (2007). Microporous carbon derived from pinecone hull as anode material for lithium secondary batteries. *Materials Letters*, *61*, 5209–5212.

Zhu, Y., Wang, S., Zhong, Y., Cai, R., Li, L., & Shao, Z. (2016). Facile synthesis of a MoO_2-Mo_2C-C composite and its application as favorable anode material for lithium-ion batteries. *Journal of Power Sources*, *307*, 552-560.